THE JOURNAL OF PHYSICAL CHEMISTRY B

Article

pubs.acs.org/JPCB

Heat Capacity Behavior and Structure of Alkan-1-ol/Alkylbenzoate Binary Solvents

Ana M. Navarro, Begoña García, Francisco J. Hoyuelos, Indalecio A. Peñacoba, S. Ibeas, and José M. Leal*

Departamento de Química, Universidad de Burgos, 09001 Burgos, Spain

Supporting Information

ABSTRACT: Heat capacities for the binary mixtures of methanol with (C_1−C_4) alkylbenzoates and methylbenzoate with (C_1−C_{11}) alkan-1-ols have been measured over the whole composition range at 298.15 K under atmospheric pressure. From the experimental measurements, the derived excess molar heat capacities and partial excess molar heat capacities at infinite dilution have been calculated. A Redlich−Kister-type equation was fitted to these data, and the fitting parameters and standard deviations have been evaluated. Likewise, the IR spectra for the same systems have been recorded as a function of composition. The sets of experimental data gathered contribute to shed light onto the solvent structure and the underlying molecular interactions between the mixture constituents. The conclusions drawn have been established in terms of solute−solvent and solvent−solvent interactions and the ensuing structural effects between the solvent constituents.

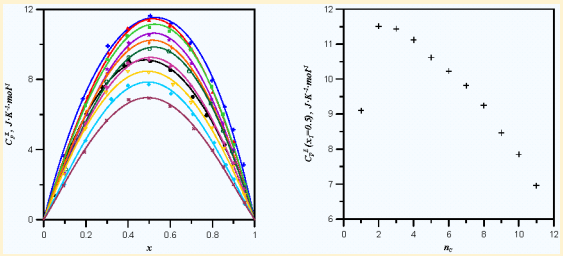

INTRODUCTION

Studies on thermodynamic and bulk properties of liquid mixtures represent a useful complementary tool to learn the structural features of the pure constituents and the interactions that govern the mixture behavior.[1] Isobaric molar heat capacity, C_P, of liquid mixtures is a key quantity in many settings; knowledge of the C_P values as a function of composition may provide valuable structural information.[2] Likewise, excess properties help to describe the effects exerted by the molecular orientation and contribute to shed light into the governing interactions.[3] Excess molar heat capacity, C_P^E, serves to quantify the structural features, to develop theoretical models[4] and to design suitable mixed solvents for industrial processes.[5]

Aromatic esters are known to display specific behavior due to self-aggregation. In particular, benzoic acid esters are categorized as an important class of solvents; the dipolar, hydrophobic behavior and the easily polarizable π-electron system afford these solvents a highly selective ability, turning them into suitable materials for a variety of applications. The liquid structure of pure alkylbenzoates has rather scarcely been investigated. Their pronounced dipole moment (~1.94 D) promotes certain molecular ordering in the pure state;[6] dipole moment and dipole−dipole interactions increase with the side-chain length. The role played by the size and molecular geometry must also be considered; long side chains give way to less planar molecules, hinder the interaction with neighbor dipoles, and result in less stable dipolar associates.[7] Pure alkylbenzoates self-aggregate by H-bonding and remain as stable dimers, the more so the shorter the side chain.[8] Pure alcohols, on the other hand, are extensively self-associated by H-bonding, the association extent decreasing for larger alcohols.[9] H-bonding determines the alcohol structure; open chains, cyclic dimers, and dimer/trimer mixtures are viable, primary alcohols displaying higher association ability due to the weaker steric hindrance of the OH group.[10,11] Other studies, however, disregard the aggregation stoichiometry, assuming equilibrium between O atoms with and without the lone electron pairs involved. Hence, H-bonding enthalpies become nearly independent of the alcohol size, and the small OH free fraction should, in turn, increase slightly for larger alcohols.[12,13]

To gain further insight into the structures of alkanol/alkylbenzoate systems[10,14,15] and analyze the size and shape effects on the excess properties, new C_P data were measured, and the excess molar heat capacities, C_P^E have been calculated at 298.15 K for methanol with methylbenzoate (MB), ethylbenzoate (EB), propylbenzoate (PB), and butylbenzoate (BB) and for MB with 11 *n*-alcohols, from methanol to undecanol. Also, the IR spectra of the corresponding binary mixtures recorded over the whole composition range have contributed to assess the structural effects of the alcohol size (n_C) and alcohol self-association ability and the ester side-chain length as well.

EXPERIMENTAL SECTION

Pure solvents, of the highest purity commercially available, were used without further purification, degassed with ultrasound, dried over Fluka 0.3 nm molecular sieves, and kept out of the light before use. The purity of the solvents was assessed by a Perkin-Elmer 990 gas chromatograph. The binary mixtures, fully miscible over the whole composition range, were prepared by mass ($\pm 10^{-5}$ g) using a Mettler AT 261 Delta Range balance, always expressing the mixture composition as *x*, the alcohol mole

Received: March 27, 2012
Revised: July 7, 2012
Published: July 11, 2012

   dx.doi.org/10.1021/jp302934b | J. Phys. Chem. B 2012, 116, 9768−9775

fraction. The samples were degassed with ultrasound and injected by syringe into suitably stoppered bottles to prevent the liquids from preferential evaporation.

Density Measurements. Densities, ρ ($\pm 5 \times 10^{-6}$ g cm^{-3}), were measured with the vibrating-tube computer-controlled DSA 5000 Anton Paar digital densitometer (Tables 1S and 2S, Supporting Information), based on the mechanical oscillator measuring principle and equipped with a Peltier element that ensures thermostatization ($\pm$0.01 K). Calibration was performed with deionized doubly distilled water (Milli-Q, Millipore) and *n*-nonane (Fluka, 99.2% GC).[14]

IR spectra. The IR spectra were recorded with a Nicolet 8700 FT-IR spectrophotometer fitted with a multireflection crystal; it is ideally suited to analyze low-concentration samples with high sensitivity and provides advanced velocity for rapid and slow scanning over the 25000−20 cm^{-1} spectral range. The analysis of the deconvolution of the ATR-FTIR spectral data in the 3750.93−2649.76 cm^{-1} range was handled using Galactic Grams/AI (version 7.01) computer program (Thermo Galactic, Salem, U.S.A.). No smoothing was conducted on the spectra to facilitate the determination of the number of overlapping bands. The spectra were truncated in the desired region, and the baseline was corrected for sloping.

Heat Capacity Measurements. Differential scanning calorimetry (DSC) is the most used technique for calorimetric measurements. Molar heat capacities were measured at atmospheric pressure with a highly sensitive ($\pm$0.01 J·mol^{-1}·K^{-1}) Setaram Micro DSCIII differential scanning calorimeter, based on the Tian-Calvet principle, which determines the change of heat flow from/to the liquid sample upon temperature scanning; the calorimetric signal is proportional to the heat capacity per unit volume. Evaluation of the C_P values of the liquid samples requires the density data of the binary mixtures.

Measuring Procedure. C_P measurements were carried out in triplicate by the isothermal step method ($\pm$0.03 J·mol^{-1}·K^{-1}), which requires only very small (1 mL) samples.[2,16,17] The instrument consists of two differentially assembled (reference and measuring) vessels lodged in a calorimetric block immersed in a thermostatting liquid (undecane) that ensures constant temperature ($\pm$0.01K);[17−20] the assembly is placed in an inert atmosphere.[18] Calibration was performed according to the Joule effect method, introducing a temperature correction.[18,21] Hexane (Fluka, >99.5%) was the reference material and butan-1-ol (Aldrich, >99.5%) the calibration liquid. The special vessels used leave out the presence of vapor, and no vapor correction was needed.[22]

The heat flow (power)/temperature rate from/to the sample was monitored versus time while programming the sample temperature.[21] Heat capacities were obtained in three steps: (i) the differential heat flow was measured with the reference and sample vessels filled up with *n*-hexane; (ii) hexane was replaced by the calibration material in the reference vessel; and (iii) hexane was replaced by the sample in the measuring vessel.[18] The calibration procedure consists of steps (i) and (ii), with C_P reference data taken from literature.[23] In each experiment, the temperature and differential heat flow rate were recorded versus time. An overall temperature increment was applied at a 0.05 K·min^{-1} scan rate. To minimize convection effects outside of the thermostatic zone, positive and negative temperature increments were settled. Heat capacities were obtained as

$$(C_P)_S = M_S \frac{[\rho_R((C_P)_R/M_R) - \rho_B((C_P)_B/M_B)]}{\rho_S} \times \frac{A_{S,B} - A_{B,B}}{A_{R,B} - A_{B,B}} + \frac{\rho_B(C_P)_B}{\rho_S M_B} \quad (1)$$

where ρ stands for the absolute density, M for the molecular weight, and A for the peak surface; subscripts S, R, and B refer to heat readings of the solvent sample, reference (1-butanol), and blank (*n*-hexane), respectively.[18]

RESULTS AND DISCUSSION

The C_P values measured for the pure constituents concurred well with literature values (Table 1). Figure 1 shows the C_P versus x plot for 11 MB−alkanol systems (Table 3S, Supporting Information). The slopes steadily switched from negative (methanol) to positive (undecanol), and only for n_C = 5−6 did the C_P values become (roughly) composition-independent; this feature is consistent with the observed variation in excess molar volumes reported earlier.[14] The observed C_P profile reflects the change in structure inherent to the distinct types of aggregates formed when the alcohol content was raised.[24] On the other hand, the four methanol + alkylbenzoate systems (Table 4S, Supporting Information) always displayed positive deviation (Figure 2); the slope of the C_P versus x plot rose with increasing ester chain length. The polynomial eq 2 was used to fit the two sets of C_P versus x data pairs (Tables 2 and 3)

$$C_P = \sum_{j=0}^{m} A_j x^j \quad (2)$$

Nonideal behavior in mixed solvents bears relation with (a) difference in size and shape between constituents, (b) molecular reorientation after mixing, and (c) molecular interactions. The extent of the mixture deviation from ideal behavior can best be described by the derived excess property, that is, the property in excess compared to an ideal solution of the same composition. The excess molar heat capacity, C_P^E, accounts for the liquid ordering upon mixing; its behavior with the mixture composition reflects the change in the solvent structure and provides a measure of the underlying interactions between constituents.[27] The C_P^E values were evaluated according to

$$C_P^E = C_P - (xC_{P_1}^0 + (1 - x)C_{P_2}^0) \quad (3)$$

where $C_{P_1}^0$ and $C_{P_2}^0$ stand for the alcohol and ester contributions, respectively. The C_P^E versus x data (Tables 5S and 6S, Supporting Information) displayed maxima at (roughly) x = 0.5 (Figures 3 and 4). The Redlich−Kister-type polynomial eq 4 was fitted to the C_P^E values (Tables 4 and 5) as a function of the mixture composition[25]

$$C_P^E = x(1 - x) \sum_{j=0}^{m} A_j(2x - 1)^j \quad (4)$$

the proper number of A_j fitting coefficients being evaluated by least-squares.[26]

Values of C_P^E have served to assess breaking/forming of H-bonding in polar and nonpolar mixtures.[28,29] For alkanol mixtures, positive C_P^E values have been ascribed to two competing effects, alcohol self-association and heteroassociation;[4,30] the latter contributes negatively to C_P^E as the alcohol size is raised, decreasing the maxima.[31] Thus, the C_P^E profile accounts for the

dx.doi.org/10.1021/jp302934b | J. Phys. Chem. B 2012, 116, 9768−9775

Table 1. Comparison of the Isobaric Molar Heat Capacity of the Pure Solvents, C_P ($J \cdot K^{-1} \cdot mol^{-1}$) at 298.15 K Obtained in This Work with Those Reported in the Literature

alkylbenzoate				1-alkanol									
MB	EB	PB	BB	C_1	C_2	C_3	C_4	C_5	C_6	C_7	C_8	C_9	C_{10}	C_{11}
218.32[a]	247.13[a]	274.04[a]	304.15[a]	81.48[a]	111.92[a]	144.98[a]	177.10[a]	208.97[a]	241.51[a]	273.91[a]	306.69[a]	339.64[a]	373.33[a]	406.65[a]
221.3[b]	246[d]	$273.42_{293.15K}$[b]	304.06[c]	81.47[b]	112.34[b]	143.87[b]	177.08[b]	208.98[b]	241.32[b] 240.40[c,e]	272.10[c]	305.55[b]	337.57[c]	370.5[c]	406.52[c]
221.299[c]	245.965[c]			81.11[c]	112.30[c]	143.90[c]	177.10[c]	208.10[c]	240.4[d]	272.1[d]	303.90[c]	337.98[e]	370.6[d]	406.52[f]
				81.109[f]	112.29[f]	143.85[f]	176.48[e]	208.1[d]	240.77[j]	272.53[e]	305.2[d]		371.18[e]	
				81.3[g]	112.03[k]	144.9[h]	176.82[l]	208.27[e]			305.25[e]		372.61[i]	
						144.61[m]							374.6[j]	

[a]This work. [b]Reference 6. [c]Reference 23. [d]Reference 44. [e]Reference 30. [f]Reference 45. [g]Reference 31. [h]Reference 46. [i]Reference 47. [j]Reference 48 [k]Reference 36. [l]Reference 2. [m]Reference 41.

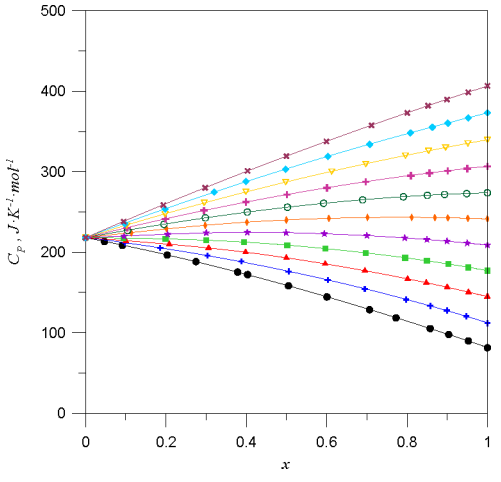

Figure 1. Molar heat capacities, C_P ($J \cdot K^{-1} \cdot mol^{-1}$), for ($x$)alkan-1-ol + (1 − x)(MB) binary solvents at 298.15 K (● methanol, + ethanol, ▲ propan-1-ol, ■ butan-1-ol, ★ pentan-1-ol, ♦ hexan-1-ol, ○ heptan-1-ol, + octan-1-ol, ▽ nonan-1-ol, ◆ decan-1-ol, × undecan-1-ol).

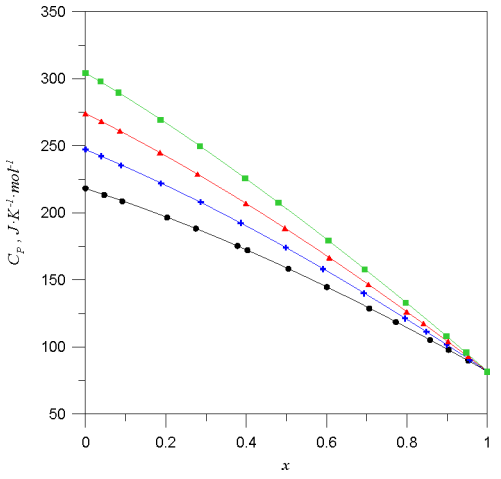

Figure 2. Molar heat capacities, C_P ($J \cdot K^{-1} \cdot mol^{-1}$), for ($x$)methanol + (1 − x)alkylbenzoate binary solvents at 298.15 K (● methylbenzoate, + ethylbenzoate, ▲ propylbenzoate, ■ butylbenzoate).

size and self-associating effects on the solvent structure and solvent association ability.[24] H-bonded alcohols raise non-randomness and nonideal behavior.[32] Moreover, dipole moments of pure esters increase as the side chain length is raised, enhancing higher ordering and stronger dipole−dipole interactions, an effect accompanied by a fall in density;[14] likewise, the planarity of short esters steadily vanishes as the side chain is raised. Hence, direct interaction between ester dipole moments is not straightforward because the larger the distance separation, the less efficient the packing, that is, geometry features must also be taken into account; the balance between dipole−dipole interaction and geometry effects exerts control of the properties of pure alkylbenzoates. The positive C_P^E values obtained over the whole composition range (Figures 3 and 4) reveal that breaking of H-bonded structures of pure alcohols upon mixing primarily contributes to C_P^E.[33,34]

Thermal relaxation inherent to complex formation between unlike molecules results in positive C_P^E values[35] and negative molar excess volumes.[14] The C_P^E curves for MB + 1-alkanol systems displayed maxima for equimolar content ($x \approx 0.5$) and decreased with a rise in the alcohol size, with only methanol

dx.doi.org/10.1021/jp302934b | J. Phys. Chem. B 2012, 116, 9768−9775

Table 2. Parameters A_j, Standard Deviation, and χ^2 Coefficients of the Polynomial Equation for Molar Heat Capacitiy, C_P, of the $\{(x)$1-Alkanol + $(1-x)$Methylbenzoate$\}$ Systems at 298.15 K

	A_0	A_1	A_2	A_3	A_4	A_5	σ	χ^2
methanol	218.06	−95.81	−49.04	8.52			0.19	4.499×10^{-1}
ethanol	218.27	−62.51	−38.21	−5.17			0.29	7.422×10^{-1}
1-propanol	218.30	−42.03	45.18	−208.82	207.47	−75.18	0.11	9.500×10^{-2}
1-butanol	218.30	−9.10	32.10	−176.70	181.60	−69.10	0.10	2.000×10^{-1}
1-pentanol	218.31	14.30	71.74	−252.58	241.54	−84.41	0.10	7.900×10^{-2}
1-hexanol	218.29	52.87	25.97	−143.99	133.59	−45.27	0.10	7.700×10^{-2}
1-heptanol	218.24	86.61	−4.45	−45.59	19.11		0.11	1.154×10^{-1}
1-octanol	218.17	119.06	−4.28	−51.84	25.72		0.19	3.157×10^{-1}
1-nonanol	218.15	153.54	−19.47	−29.20	16.75		0.23	4.682×10^{-1}
1-decanol	218.10	186.60	−31.70				0.30	9.000×10^{-1}
1-undecanol	218.02	217.89	−32.67	3.19			0.24	5.764×10^{-1}

Table 3. Parameters A_j, Standard Deviation, and χ^2 Coefficients of the Polynomial Equation for Molar Heat Capacity, C_P, of the $\{(x)$Methanol + $(1-x)$Alkylbenzoate$\}$ Systems at 298.15 K

	A_0	A_1	A_2	A_3	A_4	σ	χ^2
ethylbenzoate	247.09	−123.79	−49.43	7.84		0.19	3.764×10^{-1}
propylbenzoate	274.15	−148.78	−52.58	9.04		0.17	3.176×10^{-1}
butylbenzoate	304.30	−172.60	−79.90	50.70	−20.80	0.20	5.000×10^{-1}

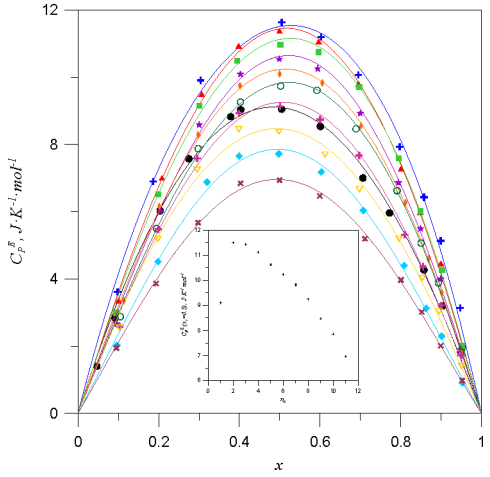

Figure 3. Molar excess heat capacities, C_P^E ($J \cdot K^{-1} \cdot mol^{-1}$), for (x)alkan-1-ol + $(1-x)$ (MB) binary solvents at 298.15 K (● methanol, + ethanol, ▲ propan-1-ol, ■ butan-1-ol, ★ pentan-1-ol, ♦ hexan-1-ol, ○ heptan-1-ol, + octan-1-ol, ▽ nonan-1-ol, ◆ decan-1-ol, × undecan-1-ol). (Inset) Plot of C_P^E ($J \cdot K^{-1} \cdot mol^{-1}$) versus alcohol size, n_C, for equimolar mixtures (x)alkan-1-ol + $(1-x)$ (MB) at 298.15 K.

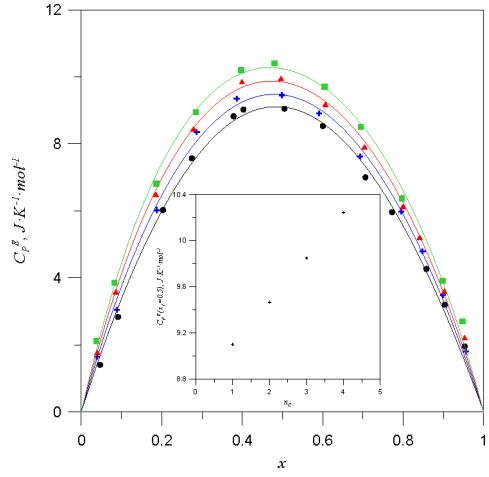

Figure 4. Molar excess heat capacities C_P^E ($J \cdot K^{-1} \cdot mol^{-1}$), for (x)methanol + $(1-x)$alkylbenzoate binary solvents at 298.15 K (● methylbenzoate, + ethylbenzoate, ▲ propylbenzoate, ■ butylbenzoate). (Inset) Plot of C_P^E ($J \cdot K^{-1} \cdot mol^{-1}$) versus the alkylbenzoate chain length n_C for equimolar mixtures (x)methanol + $(1-x)$alkylbenzoate at 298.15 K.

deviating from this trend (Figure 3). In other words, a shortening of the alcohol size causes breaking of the alcohol structure in the mixture relative to ideal behavior, raising the C_P^E value.[36] The anomalous value obtained for MB + methanol (between octanol and nonanol; Figure 3, inset) reflects the strongly H-bonded structure and pronounced proton donor ability of pure methanol; this striking feature of MB + methanol is supported by the IR data below and is consistent with the anomalous value reported earlier[14] for its internal pressure, defined as the work exerted against the cohesive forces by a liquid undergoing an isothermal expansion that entails a change in internal energy.

For methanol + alkylbenzoate mixtures, the maxima increased with a rise in the ester chain length (Figure 4, inset) (MB < EB < PB < BB), in line with the variation of C_P for pure esters, an effect ascribed to breaking of the ester dipolar ordering; likewise, the ester ability to break the methanol structure in the mixture

Table 4. Parameters, A_j, Standard Deviation, and χ^2 Coefficients of the Redlich−Kister Equation for Excess Molar Heat Capacity, C_P^E, of the $\{(x)$1-Alkanol + $(1-x)$Methylbenzoate$\}$ Systems at 298.15 K

	A_0	A_1	A_2	σ	χ^2
methanol	36.40	−2.29	−1.09	0.22	6.379×10^{-1}
ethanol	46.03	4.39	5.78	0.27	7.516×10^{-1}
propan-1-ol	45.74	3.50	−4.38	0.16	2.801×10^{-1}
butan-1-ol	44.48	4.68	−2.32	0.17	3.126×10^{-1}
pentan-1-ol	42.47	4.35	−7.16	0.17	3.079×10^{-1}
hexan-1-ol	40.91	2.63	−4.91	0.11	1.446×10^{-1}
heptan-1-ol	39.27	4.02	−5.00	0.11	1.229×10^{-1}
octan-1-ol	36.99	1.24	−6.15	0.18	3.708×10^{-1}
nonan-1-ol	33.86	−1.11	−4.14	0.22	5.239×10^{-1}
decan-1-ol	31.40	−0.86	−9.11	0.16	2.744×10^{-1}
undecan-1-ol	27.83	−0.86	−7.90	0.09	9.520×10^{-2}

dx.doi.org/10.1021/jp302934b | J. Phys. Chem. B 2012, 116, 9768−9775

Table 5. Parameters, A_j, Standard Deviation, and χ^2 Coefficients, of the Redlich−Kister Equation for the Molar Excess Heat Capacity, C_P^E, of the {(x)Methanol + (1 − x)Alkylbenzoate} Systems at 298.15 K

	A_0	A_1	A_2	σ	χ^2
ethylbenzoate	37.85	−2.93	1.98	0.19	4.294×10^{-1}
propylbenzoate	39.39	−3.78	5.10	0.15	2.783×10^{-1}
butylbenzoate	40.97	−4.16	7.71	0.23	5.762×10^{-1}

Table 6. Partial Molar Excess Heat Capacity at Infinite Dilution $\overline{C}_{P,i}^{E,\infty}$ (J·K^{-1}·mol^{-1}) for (a) {(x)1-Alkanol + (1 − x)Methylbenzoate} and (b) {(x)Methanol + (1 − x)Alkylbenzoate} Binary Solvents at 298.15 K

(a)	methylbenzoate		(b)	methanol	
	$\overline{C}_{P,1}^{E,\infty}$	$\overline{C}_{P,2}^{E,\infty}$		$\overline{C}_{P,1}^{E,\infty}$	$\overline{C}_{P,2}^{E,\infty}$
methanol	28.46	41.53	ethylbenzoate	35.45	43.45
ethanol	33.06	66.17	propylbenzoate	43.82	44.76
propan-1-ol	31.23	49.89	butylbenzoate	49.89	47.12
butan-1-ol	31.74	51.29			
pentan-1-ol	23.69	45.25			
hexan-1-ol	33.37	38.62			
heptan-1-ol	20.34	38.28			
octan-1-ol	21.46	38.13			
nonan-1-ol	20.58	36.51			
decan-1-ol	17.83	25.52			
undecan-1-ol	17.21	21.92			

increases with the ester chain length.[36] A boost in ordering upon mixing results in positive contribution to C_P^E and negative net order destruction.[37] Dispersive interactions and dipole/dipole and dipole/induced dipole attractions contribute to increased C_P^E values,[38,39] conveying the mixture propensity to nonrandomness.[40,41] Pure alkanols form strong linear and cyclic O−H−O H-bonds.[42] When alcohols mix with alkylbenzoates, unlike H-bonding associations arise, linking the alcohol OH group with the CO ester group; despite the opposed heteroassociating effect, breaking of self-associated alcohols prevails because the larger the alcohol chain, the easier the self-aggregation disruption.[8]

Partial molar functions, which account for the rate of change with concentration of extensive thermodynamic properties due to addition to a mixture of an infinitely small amount of one component, provide valuable information on binary and higher-order interactions. From the fitting coefficients of excess molar heat capacities (Tables 4 and 5), the partial excess molar property, $\overline{C}_{Pm}^E$, was evaluated for the binary constituents according to the intercept method.[15] The limiting value at infinite dilution for each constitunt, $\overline{C}_{Pm}^{E,\infty}$, obtained as the values at a mole fraction approaching zero, give a measure of the solute−solvent forces and involve geometry effects and intermolecular interactions. In addition to the intrinsic solute volume, solute−solvent forces are the main factor that governs the solvent packing around a central solute unit. Therefore, an analysis of the $\overline{C}_{Pm}^{E,\infty}$ values lends valuable insight into the solvent structure. Table 6 lists the $\overline{C}_{Pm}^{E,\infty}$ values for both constituents of the two sets investigated, showing the effect of the number of

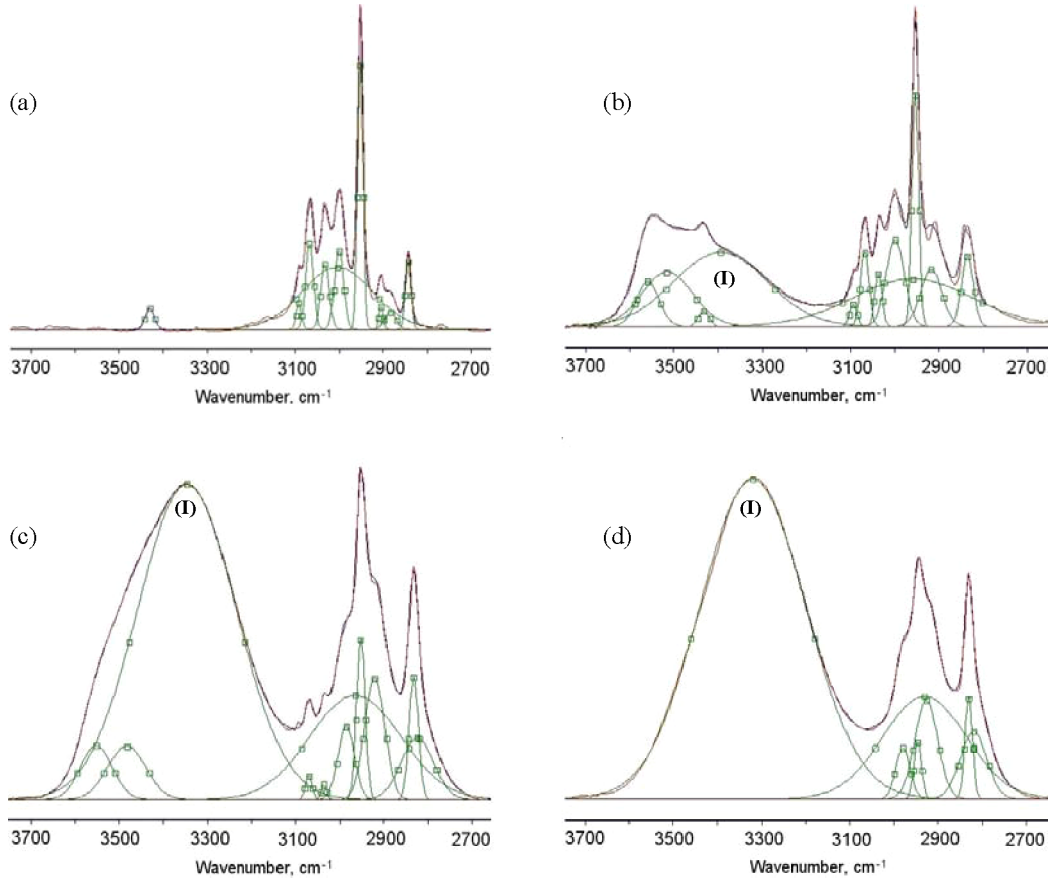

Figure 5. Deconvolution of ATR-FTIR spectra in the 3750.93−2649.76 cm^{-1} range for methanol + MB at 298.15K using Gaussian−Lorentzian functions by the GRAMS/AI program (version 7.01), (a) pure MB, (b) methanol + MB (x = 0.3309), (c) methanol + MB (x = 0.7113), and (d) pure methanol. Band (I) in the 3650−3150 cm^{-1} range shows the intermolecular association.

dx.doi.org/10.1021/jp302934b | J. Phys. Chem. B 2012, 116, 9768−9775

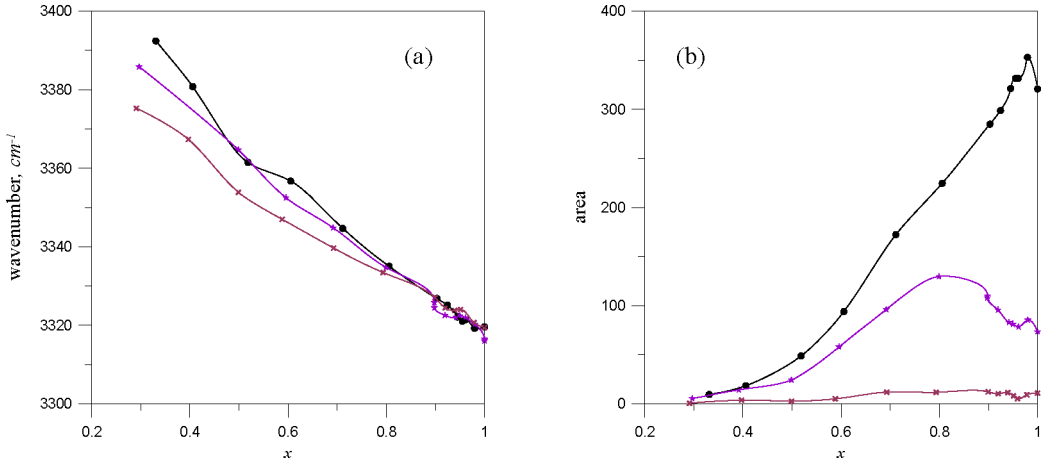

Figure 6. (a) Variation of the wavenumbers (cm^{-1}) of the peak center showing the position of the IR band (I), 3650−3150 cm^{-1}, and (b) variation of the area of the IR band (I), 3650−3150 cm^{-1} for 1-alkanol + MB systems at 298.15 K (● methanol, ★ pentan-1-ol, × undecan-1-ol).

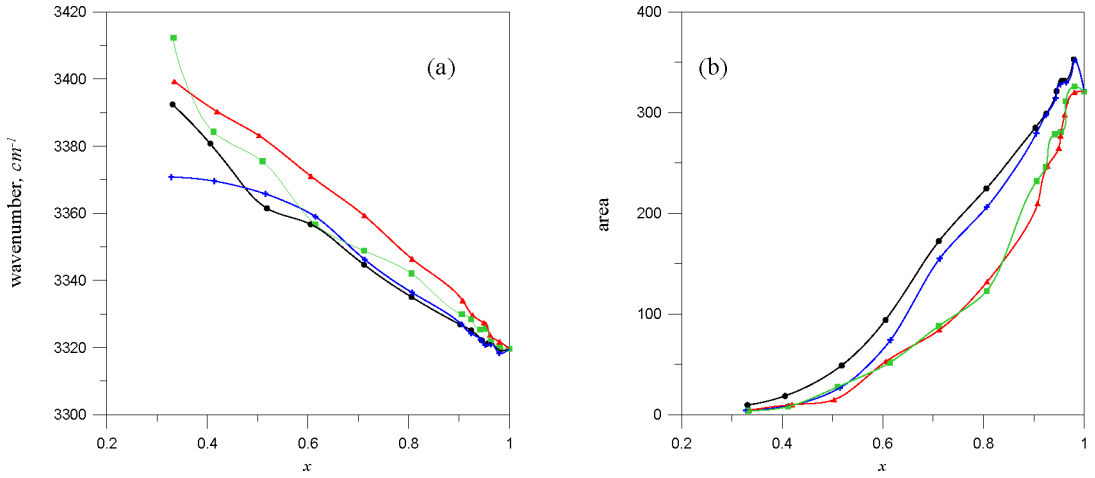

Figure 7. (a) Variation of the wavenumbers (cm^{-1}) of the peak center showing the position of the IR band (I), 3650−3150 cm^{-1} and (b) variation of the area of the IR band (I), 3650−3150 cm^{-1}, for methanol + alkylbenzoate systems at 298.15 K (● methylbenzoate + ethylbenzoate, ▲ propylbenzoate, ■ butylbenzoate).

CH_2 groups. For methanol + alkylbenzoates, the $\overline{C}_{P,1}^{E,\infty}$ and $\overline{C}_{P,2}^{E,\infty}$ contributions increased with the rise in the number of CH_2 groups of the alkyl chain. By and large, these values decreased for MB + alkanol systems when the alcohol size was raised, reflecting the propensity of polar molecules to clustering.[27]

The variation of the IR spectra for alkanol + MB and methanol + alkylbenzoate systems with increasing alcohol content, recorded over the whole composition range, are informative of homo- and heteroassociations. As an example, Figure 5 shows the variation of the IR spectra upon an increase of the alcohol content for methanol + MB. In the 3650−3150 cm^{-1} range, Figure 5 shows that for the methanol + MB system at different mole fractions, different bands are obtained from the deconvolution, passing from a very low intensity band for pure MB (Figure 5a) to four bands at intermediate mole fractions (Figure 5b and c) and to only a single, high-intensity band for pure alcohol (Figure 5d). Regarding the stretching vibration ν_{O-H}, the IR spectra recorded in the above range[43] reflect the pronounced effect of H-bonding in alcohols and is informative of alcohol association. The shift of the frequency range also reflects the bond strength and the masses involved.

Depending on the alcohol content, several subsequent bands were obtained from the deconvolution performed (Figure 5b and c). The acute band within 3650−3590 cm^{-1} is ascribed to the free OH. The band within 3600−3450 cm^{-1} corresponds to OH intramolecularly associated, whose relative intensity does not depend on the alcohol content. The wide band within 3650−3150 cm^{-1} (whose relative intensity depends on the alcohol content), denoted as (I), corresponds to the intermolecularly associated OH and involves dimer and polymer species.[43]

Figure 6a shows that the shift of the wavenumber of the peak center of band (I) for alkanol + MB depends on the alcohol size only for high ester content. Figure 7a shows that the shift of the wavenumber of the peak center of band (I) for methanol + alkylbenzoate depends on the ester side-chain length only for high ester content. Figure 6b plots the variation of the area band (I) with the alcohol content, for alkanol + MB systems, clearly disclosing the much greater area for methanol compared to pentanol and of pentanol compared to undecanol. Therefore, given that the area of this band is proportional to the concentration of intermolecular aggregates present, it follows that mixtures with methanol are much more associated. The alcohol structure is not fully distorted after mixing; though somewhat modest relative to the pure constituent, a certain alcohol association degree in the mixture still remains. Finally, Figure 7b plots the variation of the area, band (I), with alcohol

dx.doi.org/10.1021/jp302934b | J. Phys. Chem. B 2012, 116, 9768−9775

content, showing that the heteroassociation effect in methanol + alkylbenzoate systems strongly depends on the alcohol content and only very little on the ester size and ester content. All of these results concur well with the conclusions stemming from the heat capacity measurements discussed above.

CONCLUSIONS

New molar heat capacity data have been measured for alkanol/alkylbenzoate mixtures. The C_p values of the pure constituents showed a regular trend, increasing with the number of carbon atoms. The C_P^E values for the binary mixtures displayed maxima for equimolar content, and deviation from ideality is explained in terms of molecular effects, stressing the H-bonding and dipole moment effects. Breaking of self-associated alkanols is accompanied by nonspecific interactions, namely, mixing and packing effects. Three factors govern the alkan-1-ol/alkylbenzoate structures, (i) disruption of alkanol H-bonds, (ii) formation of alkanol−ester aggregates, and (iii) the shape and size factors of the components. The aggregates became weakened with an increase in the ester side-chain length and the alcohol size. The conclusions drawn are supported by the variation with the solvent composition of the IR spectra recorded.

ASSOCIATED CONTENT

Supporting Information

Tables 1S−6S, giving density, molar heat capacity, and molar excess heat capacity information. This material is available free of charge via the Internet at http://pubs.acs.org.

AUTHOR INFORMATION

Corresponding Author

*Tel.: +34 947 258819. Fax: + 34 947 258831. E-mail: jmleal@ubu.es.

Notes

The authors declare no competing financial interest.

ACKNOWLEDGMENTS

The financial support by Junta de Castilla y León, Project GR257, Ministerio de Educación y Ciencia, Project CTQ2009-13051/BQU, supported by FEDER, and Universidad de Burgos with funding by Caja de Burgos, Spain is gratefully acknowledged.

REFERENCES

(1) Comelli, F.; Bigi, A.; Vitalini, D.; Rubine, K. *J. Chem. Eng. Data* **2010**, *55*, 205−210.
(2) Zorębski, E.; Góralski, P.; Tkaczyk, M. *J. Chem. Thermodyn.* **2005**, *37*, 281−287.
(3) Checoni, R. F.; Francesconi, A. Z. *J. Solution Chem.* **2007**, *36*, 913−922.
(4) Piñeiro, A. *Fluid Phase Equilib.* **2004**, *216*, 245−256.
(5) Hanks, R. W.; Christensen, J. J. *I. Chem. Eng. Symp. Ser.* **1979**, *56*, 29−49.
(6) Riddick, J. A.; Bunger, W. B.; Sakano, T. K. *Organic Solvents. Physical Properties and Methods of Purification*, 4th ed.; Wiley: New York, 1986.
(7) Ortega, J.; Postigo, M. *Fluid Phase Equilib.* **1995**, *108*, 121−133.
(8) Hu, J.; Tamura, K.; Murakami, S. *Fluid Phase Equilib.* **1997**, *131*, 197−212.
(9) Navarro, A. M.; García, B.; Peñacoba, I. A.; Hoyuelos, F. J.; Leal, J. M. *J. Phys. Chem. B* **2011**, *115*, 10259−10269.
(10) Cerdeiriña, C. A.; Gonzalez-Salgado, D.; Romani, L.; Delgado, M. C.; Torres, L. A.; Costas, M. A. *J. Chem. Phys.* **2004**, *120*, 6648−6659.
(11) Huyskens, P. *J. Mol. Struct.* **1983**, *100*, 403−414.
(12) Souto-Caride, M.; Troncoso, J.; Losada-Pérez, P.; Peleteiro, J.; Carballo, E.; Romani, L. *Chem. Phys.* **2009**, *358*, 225−229.
(13) Rubini, K.; Francesconi, R.; Bigi, A.; Comelli, F. *Thermochim. Acta* **2007**, *452*, 124−127.
(14) García, B.; Aparicio, S.; Navarro, A. M.; Alcalde, R.; Leal, J. M. *J. Phys. Chem. B* **2004**, *108*, 15841−15850.
(15) García, B.; Alcalde, R.; Aparicio, S.; Leal, J. M. *J. Phys. Chem. B* **2005**, *109*, 19908−19914.
(16) Rudtsch, S. *Thermochim. Acta* **2002**, *382*, 17−25.
(17) Góralski, P.; Tkaczyk, M.; Chorążewski, M. *J. Chem. Eng. Data* **2003**, *48*, 492−496.
(18) Cerdeiriña, C. A.; Míguez, J. A.; Carballo, E.; Tovar, C. A.; de la Puente, E.; Romaní, L. *Thermochim. Acta* **2000**, *347*, 37−44.
(19) Cobos, J. C.; García, I.; Casanova, C.; Roux, A. H.; Roux-Desgranges, G.; Grolier, J.-P. E. *Fluid Phase Equilib.* **1991**, *69*, 223−233.
(20) Pérez-Sánchez, G.; Losada-Pérez, P.; Cerdeiriña, C. A.; Thoen, J. *J. Chem. Phys.* **2010**, *132*, 214503−1−7.
(21) Höhne, G. W. H; Hemminger, W.; Flammersheim, H.-J. *Differential Scanning Calorimetry*; Springer-Verlag: Berlin, Heidelberg, Germany, 1996.
(22) Lei, Y.; Chen, Z.; Wang, N.; Mao, C.; An, X.; Shen, W. *J. Chem. Thermodyn.* **2010**, *42*, 864−872.
(23) (a) Zábranský, M.; Ruzicka, V., Jr.; Domalski, E. S. *J. Phys. Chem. Ref. Data* **2002**, *30*, 1199−1689. (b) Zábranský, M.; Kolska, Z.; Ruzicka, V.; Domalski, E. S. *J. Phys. Chem. Ref. Data* **2010**, *39*, 013103/1−013103/404.
(24) Dzida, M.; Góralski, P. *J. Chem Thermodyn.* **2009**, *41*, 402−413.
(25) Redlich, O.; Kister, A. T. *Ind. Eng. Chem.* **1948**, *40*, 341−345.
(26) Bevington, P. *Data Reduction and Error Analysis for the Physical Sciences*; McGraw-Hill: New York, 1969.
(27) Cerdeiriña, C. A.; Tovar, C. A.; González, D.; Carballo, E.; Romaní, L. *Fluid Phase Equilib.* **2001**, *179*, 101−115.
(28) Gepert, M.; Zorebski, E.; Leszcynska, A. *Fluid Phase Equilib.* **2005**, *233*, 157−169.
(29) Patterson, D. *Thermochim. Acta* **1995**, *267*, 15−27.
(30) Calvo, E.; Brocos, P.; Piñeiro, A.; Pintos, M.; Amigo, A.; Bravo, R.; Roux, A. H.; Roux-Desgranges, G. *J. Chem. Eng. Data* **1999**, *44*, 948−954.
(31) Waliszewski, D. *J. Chem. Thermodyn.* **2008**, *40*, 203−207.
(32) Souto-Caride, M.; Troncoso, J.; Losada-Pérez, P.; Peleteiro, J.; Carballo, E.; Romani, L. *Chem. Phys.* **2009**, *360*, 106−109.
(33) Schulman, E. M.; Dwyer, D. W.; Doetschman, D. C. *J. Phys. Chem.* **1990**, *94*, 7308−7312.
(34) Wallen, S. L.; Palmer, B. J.; Garrett, B. C.; Yonker, C. R. *J. Phys. Chem.* **1996**, *100*, 3959−3694.
(35) Tanaka, R.; Nakamichi, T. *J. Chem. Thermodyn.* **1997**, *29*, 221−227.
(36) (a) Peleteiro, J.; Troncoso, J.; Gónzalez-Salgado, D.; Valencia, J. L.; Souto-Caride, M.; Romaní, L. *J. Chem. Thermodyn.* **2005**, *37*, 935−940. (b) Peleteiro, J.; Troncoso, J.; Gónzalez-Salgado, D.; Valencia, J. L.; Cerdeiriña., C. A.; Romaní, L. *Int. J. Thermophys.* **2004**, *25*, 787−803.
(37) Calvo-Iglesias, E.; Bravo, R.; Pintos, M.; Amigo, A.; Roux, A. H.; Roux-Desgranges, G. *J. Chem. Thermodyn.* **2007**, *39*, 561−567.
(38) Chorażewski, M. *J. Chem. Eng. Data* **2007**, *52*, 154−163.
(39) Baluja, S.; Matsuo, T.; Tamura, K. *J. Chem. Thermodyn.* **2001**, *33*, 1545−1553.
(40) Pardo, J. M.; Tovar, C. A.; Troncoso, J.; Carballo, E.; Romaní, L. *Thermochim. Acta* **2005**, *433*, 128−133.
(41) Peleteiro, J.; González-Salgado, D.; Cerdeiriña., C. A.; Romaní, L. *J. Chem. Thermodyn.* **2002**, *34*, 485−497.
(42) Jeffrey, G. A. *An Introduction to Hydrogen Bonding*; Oxford University Press: New York, 1997.
(43) Pretsch, E.; Clero, T; Seibl, J.; Simon, W. *Tablas para la determinación estructural por métodos espectroscópicos*, 3rd ed.; Springer: Barcelona, Spain, 2000.
(44) Lide, R. D. *CRC. Handbook of Chemistry and Physics*, 83rd ed.; CRC Press LLC: Boca Raton, FL, 2003; http://Hbcpnetbase.com/.
(45) *CDATA, Database of Thermodynamic and Transport Properties for Chemistry and Engineering*, version 1.020; Departament of Physical

Chemistry, Institute of Chemical Technology: Prague, Czech Republic, 1999.
(46) Comelli, F.; Francesconi, R.; Bigi, A.; Rubini, K. *J. Chem. Eng. Data* **2006**, *51*, 1711−1716.
(47) Dzida, M.; Góralski, P. *J. Chem. Thermodyn.* **2006**, *38*, 962−969.
(48) van Miltenburg, J. C.; Gabrielová, H.; Růžička, K. *J. Chem. Eng. Data* **2003**, *48*, 1323−1331.